



# Aqueous-phase synthesis of metal hydroxide nanoplates and platinum/nickel hydroxide hybrid nanostructures and their enhanced electrocatalytic properties



Euiyoung Jung<sup>a,1</sup>, Hee-Young Park<sup>b,1</sup>, Ahyoung Cho<sup>a</sup>, Jong Hyun Jang<sup>b</sup>, Hyun S. Park<sup>b,\*</sup>, Taekyung Yu<sup>a,\*</sup>

<sup>a</sup> Department of Chemical Engineering, College of Engineering, Kyung Hee University, Yongin, 17104, Republic of Korea

<sup>b</sup> Fuel Cell Research Center, Korea Institute of Science and Technology (KIST), Seoul, 02792, Republic of Korea

## ARTICLE INFO

### Keywords:

Metal hydroxide  
Nanoplates  
Pt/Ni(OH)<sub>2</sub>  
Hybrid nanostructures  
Hydrogen evolution reaction

## ABSTRACT

We successfully synthesized metal hydroxide (Ni(OH)<sub>2</sub> and Co(OH)<sub>2</sub>) nanoplates and platinum/nickel hydroxide hybrid nanostructures (Pt/Ni(OH)<sub>2</sub>) in an aqueous solution. Transmission electron microscopy studies of the Pt/Ni(OH)<sub>2</sub> hybrid nanostructures revealed that a number of 3 nm-sized Pt nanoparticles were well dispersed on the surface of each Ni(OH)<sub>2</sub> nanoplate. The Pt/Ni(OH)<sub>2</sub> hybrid nanostructures exhibited enhanced electrocatalytic properties due to synergistic effect of Ni(OH)<sub>2</sub> and Pt.

## 1. Introduction

Platinum (Pt) is usually used for catalyst in various electrochemical reactions including oxygen reduction reaction (ORR), ethanol and methanol oxidation reaction (EOR and MOR), and hydrogen evolution reaction (HER) due to its high activity and good electrochemical stability [1–4], but Pt is an extremely rare and expensive element. One way to address this problem is to make Pt nano-sized particles. Because catalytic reactions occur on the surface of the nanoparticles, small Pt nanoparticles under 5 nm have a higher surface to volume ratio and exhibit better efficiency in catalytic reactions [5]. Typically, Pt nanoparticles supported on carbon materials (Pt/C) are commonly used as electrocatalysts for various electrochemical reactions, due to its large surface area and high conductivity of carbon particles [6,7]. However, these carbon-supported Pt nanoparticles are able to be easily sintered into larger particles or detached from the supporting materials during the electrochemical reaction [8].

Oxide or hydroxide particles has been widely studied as new supporting materials because of their strong interaction with Pt nanoparticles [9–13]. For example, some researching groups used cerium oxide (ceria) as a supporting material, however, ceria is also expensive for industrial applications [14,15]. Most recently, Z. Tang and co-workers reported the synthesis of Pt/Ni(OH)<sub>2</sub> nanostructures consisting 1.8 nm Pt nanowires supported on 585 nm-sized Ni(OH)<sub>2</sub> nanoplates

[16]. These nanostructures exhibited a good catalytic performance and durability compared with commercial Pt/C, but the procedure required harsh reaction conditions including high pressure, long reaction time, and using toxic organic solvent. Therefore, it remains a great challenge to develop a simple and reliable route to the synthesis of hybrid nanostructures consisting of highly dispersed Pt nanoparticles supported on nanocrystalline hydroxide.

Here we report a simple, aqueous-phase route to the synthesis of metal hydroxide (Ni(OH)<sub>2</sub> and Co(OH)<sub>2</sub>) nanoplates and Pt/Ni(OH)<sub>2</sub> hybrid nanostructures consisting small Pt nanoparticles deposited on Ni(OH)<sub>2</sub> nanoplates. The synthesized Ni(OH)<sub>2</sub> and Co(OH)<sub>2</sub> nanoplates had hexagonal plate shapes and good crystallinity. Pt/Ni(OH)<sub>2</sub> hybrid nanostructures were produced by reducing PtCl<sub>4</sub><sup>2-</sup> precursor in the presence of Ni(OH)<sub>2</sub> nanoplates. The synthesized Pt/Ni(OH)<sub>2</sub> hybrid nanostructures showed enhanced electrocatalytic activity toward HER in alkaline condition likely due to synergistic effect of Ni(OH)<sub>2</sub> and Pt.

## 2. Experimental

### 2.1. Materials

Polyethyleneimine (PEI, Mw = 750,000, 50 wt% solution in water), polyvinylpyrrolidone (PVP, Mw = 55,000), nickel(II) acetate tetrahydrate (Ni(CH<sub>3</sub>COO)<sub>2</sub>·4H<sub>2</sub>O, 98%), cobalt(II) acetate (Co(CH<sub>3</sub>COO)<sub>2</sub>,

\* Corresponding authors.

E-mail addresses: [hspark@kist.re.kr](mailto:hspark@kist.re.kr) (H.S. Park), [tkyu@khu.ac.kr](mailto:tkyu@khu.ac.kr) (T. Yu).

<sup>1</sup> These authors contributed equally to this work.

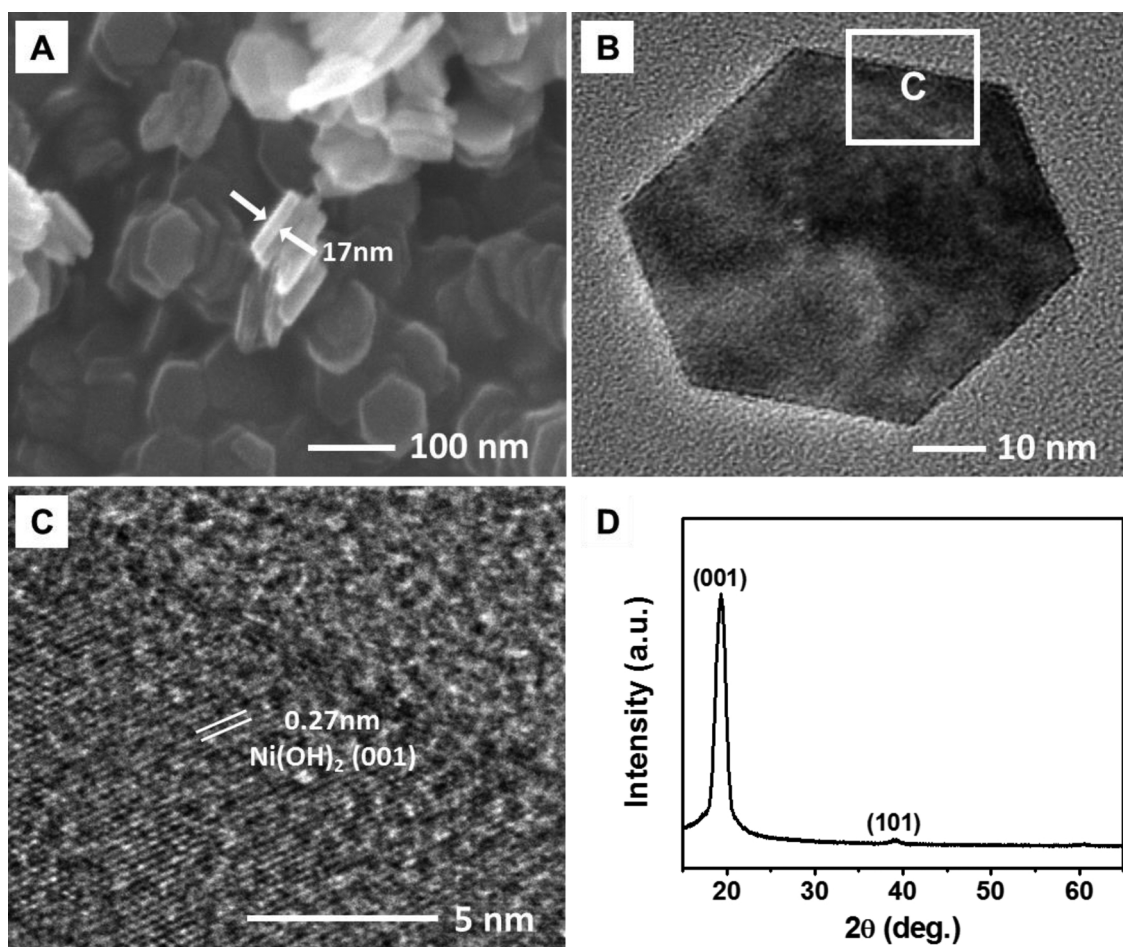


**Fig. 1.** (A) SEM, (B) TEM, and (C) HRTEM images of  $\text{Ni}(\text{OH})_2$  nanoplates synthesized by heating an aqueous solution containing  $\text{Ni}(\text{CH}_3\text{COO})_2 \cdot 4\text{H}_2\text{O}$ , PEI, and hexylamine at  $90^\circ\text{C}$  for 3 h. (D) XRD pattern of the  $\text{Ni}(\text{OH})_2$  nanoplates.

99.995%), potassium tetrachloroplatinate ( $\text{K}_2\text{PtCl}_4$ , 99.99%), hexylamine (99%), sodium borohydride ( $\text{NaBH}_4$ , 98%), ethanol (ACS reagent Plus), nafion dispersion (5 wt% in water/aliphatic alcohol), and potassium hydroxide (KOH, 99.9%) were purchased from Sigma Aldrich and utilized without further purification. Commercial Pt nanoparticle catalyst (Pt black, high surface area) was provided by Alfa Aesar.

## 2.2. Synthesis of $\text{Ni}(\text{OH})_2$ and $\text{Co}(\text{OH})_2$ nanoplates

To prepare the  $\text{Ni}(\text{OH})_2$  nanoplates, 500 mg of PEI was added into 100 mL of DI-water with 101 mg of hexylamine and heated to  $95^\circ\text{C}$  under magnetic stirring. And then, 3 mL of aqueous solution containing 249 mg of  $\text{Ni}(\text{CH}_3\text{COO})_2 \cdot 4\text{H}_2\text{O}$  was rapidly injected in the solution. After 3 h, the resulting solution was centrifuged and dispersed in 5 mL DI-water. To prepare the  $\text{Co}(\text{OH})_2$  nanoplates, 177 mg of  $\text{Co}(\text{CH}_3\text{COO})_2$  was used instead of  $\text{Ni}(\text{CH}_3\text{COO})_2 \cdot 4\text{H}_2\text{O}$ .

## 2.3. Synthesis of Pt/ $\text{Ni}(\text{OH})_2$ hybrid nanostructures

1 mL aqueous dispersion of  $\text{Ni}(\text{OH})_2$  nanoplates was mixed with 9 mL of aqueous solution containing 20 mg of PVP and various amount of  $\text{K}_2\text{PtCl}_4$  (5, 10, 15 and 21 mg, respectively). After the solution was heated in  $95^\circ\text{C}$  for 20 min, 1 mL solution containing 4 mg of  $\text{NaBH}_4$  was injected into the solution. After heating the reacting solution at same temperature for 30 min, the product was separated by centrifugation and then dispersed in DI-water.

## 2.4. Characterization

Transmission electron microscopy (TEM) and high-resolution TEM (HRTEM) images were captured using a JEM-2100F microscope operating at 200 KV or a FEI Titan transmission electron microscope. STEM images were obtained using a FEI Titan transmission electron microscope. Scanning electron microscopy (SEM) images were obtained using a Jeol JSM-6701F. Powder X-ray diffraction (XRD) patterns were obtained with a D8-Advances (Bruker AXS) diffractometer, equipped with a rotating anode and a  $\text{CuK}\alpha$  radiation source ( $\lambda = 0.154\text{ nm}$ ). The atomic ratio of Pt/ $\text{Ni}(\text{OH})_2$  hybrid nanostructures was measured using a direct reading Echelle inductively coupled plasma (ICP) spectrometer. X-ray photoelectron spectra (XPS) were obtained using a K-Alpha<sup>TM</sup> X-ray Photoelectron Spectrometer (Thermo Fisher Scientific).

## 2.5. Electrochemical analysis

Electrochemical analysis was carried out using a rotating disk electrode system (PINE) and a conventional three-electrode setup. Electrode potential was controlled by an Autolab potentiostat (EcoChemi). Catalyst coated rotating disk electrode (RDE), saturated calomel electrode, and platinum wire served as the working, reference, and counter electrode, respectively. To make working electrode, fine dispersion of catalyst powder was obtained using an ultrasonic treatment while temperature of the ultrasonic bath maintained under around  $23^\circ\text{C}$ . An adequate amount of the dispersion was pipetted onto the glassy carbon disk of a RDE to achieve Pt loading of  $0.0766\text{ mg}_{\text{Pt}}\text{ cm}^{-2}$  and dried under an air atmosphere. Then, a  $5\text{ }\mu\text{L}$  of

diluted Nafion dispersion in 1-propanol (1/10 by v/v) was pipetted onto the catalyst and dried under an air atmosphere.

Hydrogen evolution reaction (HER) polarization was measured in a H<sub>2</sub>-saturated 0.1 M KOH (21 °C) with a RDE rotation speed of 1600 rpm and scan rate of 20 mV s<sup>-1</sup>. Before the measurement, cyclic voltammetry was conducted in an Ar-saturated 0.1 M KOH (21 °C) between 0.05 and 1.00 V for 5 times at a scan rate of 20 mV s<sup>-1</sup> to obtain stable catalyst surfaces. The ECSA<sub>Pt</sub> of catalyst was determined using a hydrogen desorption charge observed in cyclic voltammetry (Fig. S4) and the charge density of hydrogen desorption on polycrystalline Pt surfaces (0.21 mC cm<sup>-2</sup>). Briefly, ECSA<sub>Pt</sub> is  $Q_{\text{Hupd}}/0.21C \text{ cm}_{\text{Pt}}^{-2}$  where  $Q_{\text{Hupd}}$  is determined from the proton desorption charge in CV curves.  $Q_{\text{Hupd}}$  is calculated from anodic peak area at 0.05–0.5 V subtracted by the double layer charging capacitance at the same potential window considering the scan rate (0.02 V s<sup>-1</sup>).

### 3. Results and discussion

#### 3.1. Characterization of Ni(OH)<sub>2</sub> and Co(OH)<sub>2</sub> nanoplates

In this study, Ni(OH)<sub>2</sub> and Co(OH)<sub>2</sub> nanoplates were synthesized by heating an aqueous solution containing metal cation, PEI, and hexylamine at 95 °C for 3 h [17,18]. As shown in Fig. 1, A and B, the product mainly contained nanoparticles in a hexagonal plate shape with lateral dimensions of 45 nm and a thickness of 17 nm. A HRTEM image indicates that the top and bottom planes of the nanoplates were enclosed by (001) planes (Fig. 1C). Powder XRD pattern of the product shows a strong diffraction peak at 19.2° and a relatively weak peak at 39.2°, which can be indexed to (001) and (101) reflections of the hexagonal closed packed β-Ni(OH)<sub>2</sub> (Fig. 1D,  $a = 3.126 \text{ \AA}$  and  $c = 4.605 \text{ \AA}$ , Joint Committee on Powder Diffraction Standards (JCPDS) file no. 14-0117), respectively. In the JCPDS file, the intensity ratio of  $I_{(001)}/I_{(101)}$  is about 1. The peak intensity ratio of the synthesized Ni(OH)<sub>2</sub> nanoplates was as high as 23.6, suggesting that the nanoplates grow mainly along the <001> direction. Co(OH)<sub>2</sub> hexagonal nanoplates were also synthesized by using Co(CH<sub>3</sub>COO)<sub>2</sub> as a precursor instead of Ni(CH<sub>3</sub>COO)<sub>2</sub>·4H<sub>2</sub>O while keeping other experimental condition unchanged. Fig. S1, A and B show typical SEM and TEM images of the sample, indicating the formation of hexagonal nanoplates with sizes of around 500 nm and a thickness of 45 nm. The powder XRD pattern taken from the nanoplates shows the presence of diffraction peaks at 19.1° and 38.0° which can be assigned to (001) and (011) plane of hcp Co(OH)<sub>2</sub> ( $a = 3.182 \text{ \AA}$  and  $c = 4.658 \text{ \AA}$ , JCPDS file no. 74-1057), respectively (Fig. S1C). The high intensity ratio of  $I_{(001)}/I_{(011)}$  and diffraction spots with a six-fold rotational symmetry in ED patterns taken by a single hexagonal nanoplate also demonstrate that the top and bottom planes of the Co(OH)<sub>2</sub> nanoplates were enclosed by (001) planes (Fig. S1, B and C).

#### 3.2. Characterization of Pt/Ni(OH)<sub>2</sub> hybrid nanostructures

The synthesized Ni(OH)<sub>2</sub> nanoplates were then used as supports for the preparation of Pt/Ni(OH)<sub>2</sub> hybrid nanostructures. Pt nanoparticles were directly synthesized on the surface of the Ni(OH)<sub>2</sub> nanoplates upon reduction of Pt precursor in the presence of PVP as a stabilizer for the overall Pt/Ni(OH)<sub>2</sub> hybrid nanostructures. Fig. 2A shows a typical TEM image of the Pt[1]/Ni(OH)<sub>2</sub> hybrid nanostructures, indicating that a number of Pt nanoparticles were well dispersed on the surface of each Ni(OH)<sub>2</sub> nanoplate. The number in the square brackets indicates the relative amounts of Pt precursors used in the synthesis. HRTEM image of a single nanostructure shows the formation of Pt nanoparticles with sizes of 3 nm on a Ni(OH)<sub>2</sub> nanoplate (Fig. 2B). The Pt nanoparticles were well dispersed on the surface of the nanoplate without significant overlap between them. From the XPS analysis, it was confirmed that the reduction of Pt precursor during the synthesis hardly altered the chemical state of Ni(OH)<sub>2</sub> (Fig. S2). The overall weight percentage of Pt in

the Pt[1]/Ni(OH)<sub>2</sub> nanostructures was as high as 66.7%, which was measured by inductively coupled plasma-mass spectrometry (ICP-MS) measurements. In the previous report on the synthesis of Pt/CeO<sub>2</sub> hybrid nanostructures, it was reported that the electrostatic attraction between the positively charged surface of the CeO<sub>2</sub> nanoparticles and the negatively charged PtCl<sub>4</sub><sup>-</sup> precursor played a key role for the formation of the hybrid nanostructures [19]. In the present synthesis, the zeta potential value of the Ni(OH)<sub>2</sub> nanoplates was as high as 29.6 mV at pH = 6.45, which would be enough to attach PtCl<sub>4</sub><sup>-</sup> on their surface (Fig. S3). To increase the Pt amount in the nanostructures, syntheses were performed by using increased amount of Pt precursor. Fig. 2, C to E shows TEM images of the Pt/Ni(OH)<sub>2</sub> hybrid nanostructures synthesized using 2, 3 and 4.2 times as much Pt precursor compared with the sample shown in Fig. 2A, respectively. By increasing the amount of Pt, the Pt nanoparticles were enlarged and covered the surface of Pt/Ni(OH)<sub>2</sub> nanoplates, like as core/shell structures (Fig. 2E). In addition, the weight percentages of Pt in the nanostructures were 77.9, 81.9 and 81.8%, respectively. The Pt loading of around 82% seemed to be the maximum Pt supported on Ni(OH)<sub>2</sub> plate and it agrees well with expected Pt weight percent (80.7%) of 4 nm thick Pt films on both side of 10 nm thick Ni(OH)<sub>2</sub> plate. The electrochemical active surface area of Pt in Pt/Ni(OH)<sub>2</sub> measured in cyclic voltammetry also shows similar trend to that of the weight percentages (Fig. S4).

As also shown in Fig. 1, Ni(OH)<sub>2</sub> nanoplate surfaces are highly covered by Pt nanoparticles with the 66.7 wt% of Pt and further increase of Pt loading seemed to insignificantly increase the interfaces between Pt and Ni(OH)<sub>2</sub>. This result implies that chemical reduction of adsorbed PtCl<sub>4</sub><sup>2-</sup> on Ni(OH)<sub>2</sub> dominates Pt deposition process, and the maximum catalyst amount layered on Ni(OH)<sub>2</sub> is limited by the surfaces of Ni(OH)<sub>2</sub> supports. XRD patterns after the attachment of Pt nanoparticles on Ni(OH)<sub>2</sub> nanoplates show the presence of diffraction peaks at 19.2° and 39.3°, indicating (001) plane of Ni(OH)<sub>2</sub> and (111) plane of Pt, respectively (Fig. 2F).

#### 3.3. Electrochemistry of Pt/Ni(OH)<sub>2</sub> hybrid nanostructures

To address synergistic effect of Pt and Ni(OH)<sub>2</sub>, HER polarization was measured using a rotating disk electrode (RDE) system (Fig. 3). Because the Ni(OH)<sub>2</sub> had been reported to enhance the HER activity of Pt in alkaline condition presumably via promoting water activation [20,21], it was expected that the Pt/Ni(OH)<sub>2</sub> hybrid nanostructures showed improved HER activity [9]. The Ni(OH)<sub>2</sub> promotes the kinetics of rate determining step of HER on Pt surfaces, such as water dissociative adsorption process in the basic electrolyte, resulting in the improve HER activity [9]. In 0.1 M KOH solution, the Pt/Ni(OH)<sub>2</sub> presents decreased overpotentials for the HER than commercial Pt black catalyst (Fig. 3A). Pt mass specific activity of Pt/Ni(OH)<sub>2</sub> hybrid nanostructures are also higher by 26.2 – 38.8% than that of commercial Pt black catalyst (Fig. 3B). However, Pt/Ni(OH)<sub>2</sub> showed decreased mass specific activity with the increased Pt weight composition in Pt/Ni(OH)<sub>2</sub>. As the interface Pt and Ni(OH)<sub>2</sub> is insignificantly increased with the increased Pt loading amounts, the inverse proportion of mass normalized HER activity to Pt loading amount indicates the higher HER activity of Pt/Ni(OH)<sub>2</sub> in the presence of the interfaces of Pt and Ni(OH)<sub>2</sub> rather than the bulk Pt surface. In addition, the Ni(OH)<sub>2</sub> plates were dimensionally stable at a wide range of electrochemical potential. TEM and energy dispersive spectroscopy (EDS) mapping images of Pt/Ni(OH)<sub>2</sub> clearly show unchanged hexagonal Ni(OH)<sub>2</sub> plates that decorated with Pt nanoparticles after the HER experiments (10 potential cycling between -0.2 V and 1.0 V) (Fig. S5).

### 4. Summary

In summary, we demonstrated new synthetic routes to synthesize metal hydroxide nanoplates and Pt/Ni(OH)<sub>2</sub> hybrid nanostructures in an aqueous-phase. The Pt/Ni(OH)<sub>2</sub> hybrid nanostructures exhibited

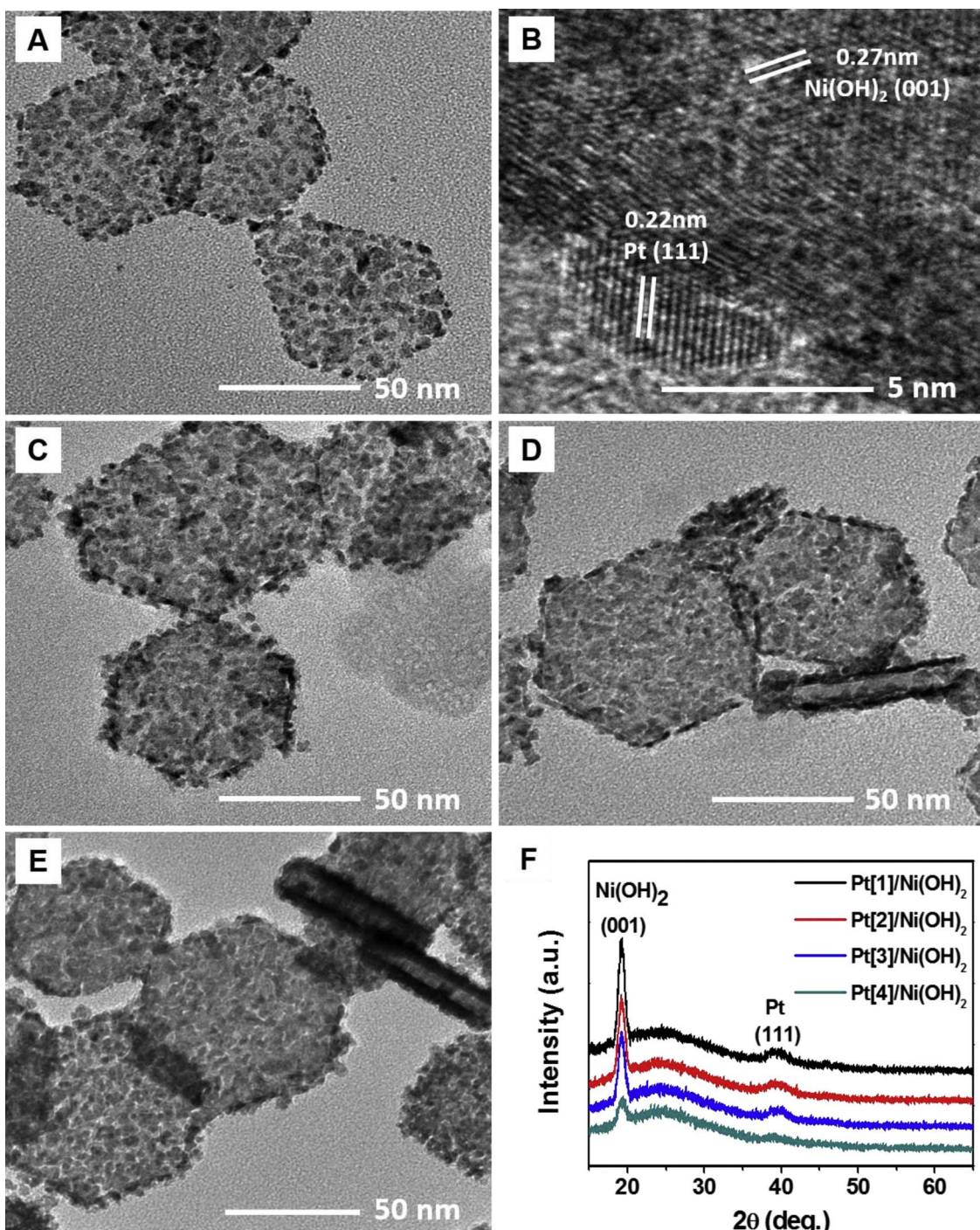


**Fig. 2.** TEM and (B) HRTEM images of Pt[1]/Ni(OH)<sub>2</sub> hybrid nanostructures produced by reducing PtCl<sub>4</sub><sup>2-</sup> precursor in the presence of the Ni(OH)<sub>2</sub> nanoplates. (C to E) TEM images of Pt[X]/Ni(OH)<sub>2</sub> (X = 2, 3, and 4.2) hybrid nanostructures synthesized under the same conditions as those in Fig. 2A except that the reaction was conducted with the increased Pt salt by 2, 3, and 4.2 times, respectively, as indicated in the square brackets. (F) XRD patterns of the Pt/Ni(OH)<sub>2</sub> hybrid nanostructures.

substantially enhanced electrocatalytic performance towards HER compared with commercial Pt black catalysts indicating synergistic effect of Pt and Ni(OH)<sub>2</sub> nanoplates. In addition, the Pt/Ni(OH)<sub>2</sub> hybrid nanostructures were dimensionally stable under the HER conditions. The key of this research is that we can easily make improved electrochemical catalysts in an aqueous-phase. The present synthesis is really simple and do not require harsh reaction conditions including high pressure, long reaction time, and using toxic organic solvent. We believe that our results are also important to guide the design of more active catalysts for fuel cells and other applications.

#### Acknowledgement

This research was supported by the Basic Science Research Program through the National Research Foundation of Korea (NRF) funded by the Ministry of Science, ICT & Future Planning (2014R1A5A1009799) and by the National Research Foundation of Korea (NRF) grant funded by the Korea government (MSIP) (NRF-2015R1C1A1A01054109, NRF-2016R1E1A2A01939795, and NRF-2016M3D1A1021140).

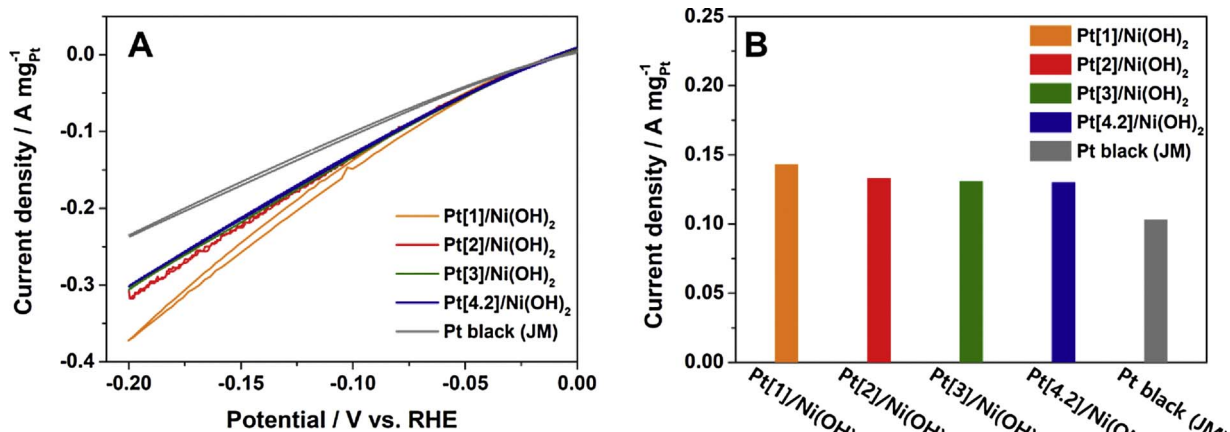


**Fig. 3.** (A) HER polarization and (B) Pt mass specific activity of Pt/Ni(OH)<sub>2</sub> and commercial Pt black catalysts measured at 0.1 V with different catalyst loadings on Ni(OH)<sub>2</sub>. The number in the square brackets indicates the relative amounts of Pt precursors used in the synthesis. Polarization curves were recorded in 0.1 M KOH aqueous electrolyte solution with a scan rate of 20 mV s<sup>-1</sup> and a RDE rotation speed of 1600 rpm.

## Appendix A. Supplementary data

Supplementary data associated with this article can be found, in the online version, at <https://doi.org/10.1016/j.apcatb.2017.11.054>.

## References

- [1] Z. Peng, H. Yang, Nano Today 4 (2009) 143–164.
- [2] E. Formo, Z. Peng, E. Lee, X. Lu, H. Yang, Y. Xia, J. Phys. Chem. C 112 (2008) 9970–9975.
- [3] Y. Hu, P. Wu, Y. Yin, H. Zhang, C. Cai, Effects of structure, composition, and carbon support properties on the electrocatalytic activity of Pt-Ni-graphene nanocatalysts for the methanol oxidation, Appl. Catal. B-Environ. 111–112 (2011) 208–217.
- [4] S. Zhang, Y. Shao, G. Yin, Y. Lin, Self-assembly of Pt nanoparticles on highly graphitized carbon nanotubes as an excellent oxygen-reduction catalyst, Appl. Catal. B-Environ. 102 (2011) 372–377.
- [5] M. Shao, A. Peles, K. Shoemaker, Nano Lett. 11 (2011) 3714–3719.
- [6] Z. Zhou, Z. Huang, D. Chen, Q. Wang, N. Tian, S. Sun, Angew. Chem. Int. Ed. 49 (2010) 411–414.
- [7] J. Park, H. Wang, M. Vara, Y. Xia, ChemSusChem 9 (2016) 2855–2861.
- [8] F.J. Perez-Alonso, C.F. Elkjaer, S.S. Shim, B.L. Abrams, I.E.L. Stephen, I. Chorkendorff, J. Power Sources 196 (2011) 6085–6091.
- [9] R. Subbaraman, D. Tripkovic, K. Chang, D. Strmcnik, A.P. Paulikas, P. Hirunsit, J. Greeley, V. Stamenkovic, N.M. Markovic, Nat. Mater. 11 (2012) 550–557.
- [10] N. Cheng, M.N. Banis, J. Liu, A. Riese, X. Li, R. Li, S. Ye, S. Knights, X. Sun, Adv. Mater. 27 (2015) 277–281.
- [11] I.E. Beck, V.I. Bukhtiyarov, I.Y. Pakharukov, V.I. Zaikovsky, V.V. Kriventsov, V.N. Parmon, J. Catal. 268 (2009) 60–67.
- [12] L.A. Estudillo-Wong, Y. Luo, J.A. Diaz-Real, N. Alonso-Vante, Enhanced oxygen reduction reaction stability on platinum nanoparticles photo-deposited onto oxide-carbon composites, Appl. Catal. B-Environ. 187 (2016) 291–300.
- [13] T. Nguyen, V.T.T. Ho, C. Pan, J. Liu, H. Chou, J. Rick, W. Su, B. Hwang, Synthesis of Ti<sub>x</sub>Mn<sub>0.3</sub>O<sub>2</sub> supported-Pt nanodendrites and their catalytic activity and stability for oxygen reduction reaction, Appl. Catal. B-Environ. 154–155 (2014) 183–189.
- [14] Y. Zhou, C.L. Menendez, M.J.-F. Guinel, E.C. Needels, I. Gonzalez-Gonzalez, D.L. Jackson, N.J. Lawrence, C.R. Cabrera, C.L. Cheung, RSC Adv. 4 (2014) 1270–1275.
- [15] P. Trigads, J. Parrondo, V. Ramani, Chem. Comm. 47 (2011) 11549–11551.
- [16] H. Yin, S. Zhao, K. Zhao, A. Muqsit, H. Tang, L. Chang, H. Zhao, Y. Gao, Z. Tang, Nat. Comm. 6 (2015) 6430–6437.
- [17] J. Chung, H. Moon, S.H. Bhang, W.-S. Kim, K.W. Bong, T. Yu, J. Ind. Eng. Chem. 36 (2016) 59–65.
- [18] E. Jung, H.J. Moon, T.-J. Park, K.W. Bong, T. Yu, Sci. Adv. Mater. (2017).
- [19] T. Yu, J. Zeng, B. Lim, Y. Xia, Adv. Mater. 22 (2010) 5188–5192.
- [20] R. Subbarman, D. Tripkovic, D. Strmcnik, K. Chang, M. Uchimura, A.P. Paulikas, V. Stamenkovic, N.M. Markovic, Science 334 (2011) 1256–1260.
- [21] S.H. Ahn, S.J. Yoo, H.-J. Kim, D. Henkensmeier, S.W. Nam, S.-K. Kim, J.H. Jang, Anion exchange membrane water electrolyzer with an ultra-low loading of Pt-decorated Ni electrocatalyst, Appl. Catal. B-Environ. 180 (2016) 674–679.